Infrared Physics & Technology 127 (2022) 104380

Contents lists available at ScienceDirect

Infrared Physics and Technology

journal homepage: www.elsevier.com/locate/infrared

Regular article

Experimental and numerical study of the emissivity of rolled aluminum

M. Sainz-Menchón [a], J. Gabirondo-López [a], I. González de Arrieta [a,b], T. Echániz [c,*], G.A. López [a]

[a] Physics Department, University of the Basque Country (UPV/EHU), E-48940 Leioa, Spain
[b] CNRS, CEMHTI UPR3079, Univ. Orléans, F-45071 Orléans, France
[c] Applied Mathematics, University of the Basque Country (UPV/EHU), E-48013 Bilbao, Spain

ARTICLE INFO

Keywords:
Aluminum
Infrared emissivity
Optical properties
Surface state
Rigorous coupled-wave analysis

ABSTRACT

Directional spectral emissivity measurements on a rolled aluminum sheet are reported between 423 and 823 K in vacuum. The results are compared to available literature data and to theoretical predictions, revealing the crucial role of the surface state in explaining the observed scatter of values. In particular, it is argued that the cold-rolling process induces a multi-scale roughness profile that significantly enhances emission at all wavelengths, a phenomenon that can be described using rigorous coupled-wave analysis (RCWA). A small peak in the *p*-polarized component at oblique angles is formed by the native oxide layer. Aside from the intrinsic value of the emissivity data for the application of thermographic techniques to rolled aluminum materials, the results contained in this work also serve to validate the usefulness of RCWA to simulate the emissivities of randomly rough metal surfaces, highlighting directions of further research.

1. Introduction

Aluminum and its alloys are the most widely used light metals due to their favorable properties, such as cost, electrical conductivity, and corrosion resistance. These materials are adaptable to many applications, from household appliances to aeronautics. Many of these applications rely on developing appropriate metallurgical properties during processing, such as extrusion or rolling, for which non-contact temperature measurement is often a necessity [1]. Moreover, finished aluminum products can also require thermographical monitorization during applications, either to determine temperature distributions or for the detection of structural defects [2].

Non-contact temperature measurements in metals are particularly complicated because of their low and highly variable emissivities. For aluminum and its alloys, variations in the particular composition and surface quality can lead to unacceptably large uncertainties, if they are not tightly controlled [1]. Several sources for the normal spectral emissivity of pure aluminum exist in the literature, with notable variations that can be mostly attributed to differences in surface state [3–8]. Total hemispherical data, obtained using calorimetric methods, also show important differences, even among polished samples [9–11]. The intrinsic optical properties of pure Al have been studied systematically, and phenomenological models are available as a function of wavelength and temperature [12–14]. Nevertheless, as for many other metals, widely scattered values can be found in the literature.

Besides, the effect of surface roughness on emissivity can take complicated forms. It is often described as a three-regime phenomenon, where very low roughnesses can be accounted for by diffraction theory and very large ones by geometrical optics [5,15]. However, the intermediate range, which is the one most relevant for many applications, requires a more sophisticated approach to the electromagnetic problem. Among the many tools that can be used to analyze scattering and absorption, rigorous coupled-wave analysis (RCWA) has been used extensively to model the optical response of complex geometries, mainly for periodic structures [16,17]. However, this method can also be applied to more general surfaces, provided that the surface profile is large enough to avoid introducing spurious features in the results by enforcing periodic boundary conditions. In the particular case of aluminum, this approach has been used to model the bidirectional reflectance distribution function of samples with random rough surfaces [18].

This work presents a combined experimental and numerical investigation of the emissivity of pure aluminum. Directional spectral emissivity data for aluminum are reported for the first time in the mid-infrared range. In order to explain the measured emissivity behavior, the effects of a particular surface roughness profile (cold rolling) and of the native oxide layer have been taken into account. The use of a high-purity sample in a vacuum allows isolating the effects of roughness. The theory has been tested on normal spectral emissivity measurements of a cold-rolled aluminum sample in the relevant temperature range for non-contact temperature applications (423–823 K). The use of a linear polarizer allows an investigation into the polarized nature of the directional emissivity of the sample and the influence of the oxide

* Corresponding author.
E-mail address: telmo.echaniz@ehu.es (T. Echániz).

https://doi.org/10.1016/j.infrared.2022.104380
Received 14 March 2022; Received in revised form 21 September 2022; Accepted 27 September 2022
Available online 3 October 2022

layer. The results presented in this work are representative of realistic surface states of industrial Al materials, while the numerical method is not constrained in its application and can be generalized to other random rough surfaces.

2. Materials and methods

2.1. Experimental methods

A 50 mm × 50 mm rolled aluminum sample was purchased from Goodfellow, with a thickness of 3 mm and 99.999% purity. The directional spectral emissivity of the sample was measured using the HAIRL emissometer of the University of the Basque Country, which can perform emissivity measurements up to 1273 K in a controlled atmosphere [19]. The emissometer consists of a Bruker IFS 66v/S vacuum FTIR spectrometer, an Isotech Pegasus R blackbody used as a reference, a sample chamber that allows controlling the atmosphere and an optical entrance that selects between the blackbody and the sample radiation. Standard mid-infrared optics (Ge/KBr beamsplitter, KBr windows and DTLaGS detector) have been used in these experiments. The sample temperature was measured using two Type K thermocouples installed at 5 mm from the measurement spot. Measurements were performed in high vacuum ($5 \cdot 10^{-5}$ hPa) from 423 K to 823 K. An extensive revision of the uncertainty budget of this instrument as a function of temperature and wavelength for metallic and ceramic materials is available [19]. For pure metals at moderate temperatures, the uncertainty is dominated by the sample temperature at shorter wavelengths and by the sample surroundings and room-temperature blackbody reference at longer ones. Combined standard uncertainties (shown as shades in the figures) increase at low temperatures and long wavelengths, from a minimum value of 2% up to 28%. In the case of the lowest measured temperature (423 K) at long wavelengths, the relative combined standard uncertainty reaches values up to 97% because of the exceedingly low emissivity. These data can be numerically integrated to obtain the total hemispherical emissivities, which are relevant for heat transfer calculations. An extrapolation procedure was used to account for radiation outside the measured spectral range, while their uncertainties were obtained by propagation through a Monte Carlo random-number procedure [19]. Finally, and for the first time in this apparatus, measurements with a linear polarizer were carried out to investigate the angular dependence of the s and p components [20,21].

The surface state of the sample and the associated roughness parameters were analyzed by a Mitutoyo SJ-201 mechanical profilometer in several directions, to account for the anisotropy of the profile. These roughness measurements were conducted at a point close to, but outside the measuring spot. The parameters measured before and after the emissivity measurements were carried out were similar, indicating that heating the sample up to 823 K did not significantly alter the profile. The sample surface was further studied by scanning electron microscopy (SEM). Secondary-electron images were taken at 20 kV with a JEOL JSM-6400 microscope. Energy-dispersive X-ray spectroscopy (EDS) revealed the presence of a small amount of oxide which could not be accurately quantified with this method. Even though the sample was studied in vacuum, a slight growth in the native oxide layer of aluminum was expected. An X-ray photoelectron spectroscopy (XPS) depth profile was performed to estimate the thickness of the layer, using a SPECS system equipped with a Phoibos 150 1D-DLD analyzer and a monochromatic Al K_α source. The depth profile was obtained by Ar^+ sputtering and thickness values were determined from sputtering times by comparison to a Ta_2O_5 reference.

Table 1
Roughness parameter values of the sample as a function of angle with respect to the rolling direction. R_a stands for the average roughness, R_q for the root-mean-square roughness, R_z for the average maximum height of the profile, and RSm for the mean spacing between profile elements.

Angle/°	R_a/μm	R_q/μm	R_z/μm	RSm/μm
0	0.39	0.49	2.32	216
45	0.30	0.34	0.94	415
90	0.33	0.47	4.07	96

2.2. Numerical simulations

The emissivity of the sample was numerically investigated using rigorous coupled-wave analysis (RCWA) [16]. The calculations were made using the open-source library available in Ref. [22]. Although this approach is only valid for periodic structures, it can be easily implemented for randomly rough profiles by applying periodic boundary conditions to irregular repeating units much longer than the wavelength [18]. The roughness profiles were discretized using 100 layers of 0.01 μm thickness, which corresponds to the resolution of the profilometer. A 1-mm thick homogeneous aluminum layer was used as the bottom layer in the calculation.

The optical model of Hüttner was used to obtain the dielectric function of Al as a function of temperature [13]. This parameterization accounts for the free-electron and interband conductivities, with temperature dependence introduced through the electrical resistivity and volume expansion. The amplitudes of the two interband transitions had to be swapped to obtain the values reported by the author.

The angle of incidence was fixed to 10° to approximate the near-normal experimental results and the emissivity spectra were calculated using 35 harmonics for all wavelengths. A relative error of 3% was estimated by comparison to select calculations made with 45 harmonics. All the calculations have been executed on a single machine with an Intel Core i9-10900 CPU @2.80 GHz and 64 GB RAM.

3. Results and discussion

3.1. Experimental results

As is the case for rolled samples, the roughness profile is anisotropic. The average results of the roughness characterization are shown in Table 1. The measured profile in directions of 0°, 45° and 90° to the rolling direction is also shown in Fig. 1. It is characterized by a multi-scale nature, with small short-range roughness interspersed with deeper valleys with a larger periodicity. These cavities are typical of rolled samples and heavily influence their emissivities [23].

An SEM image of the surface of the aluminum sample is shown in Fig. 2. No contamination was found on the surface, with only a small oxygen signal being detected. The roughness profile corresponds to the standard one of rolled metals, with a well-defined rolling direction.

Directional spectral emissivity measurements were performed with the rolling direction located at 45° with respect to the rotation axis. Fig. 3 shows the near-normal emissivity spectrum of aluminum at five temperatures. As predicted by the electromagnetic theory, the emissivity of metals is low and increases at higher temperatures and shorter wavelengths [24]. Values well below 0.1 are typical of good conducting pure metals [25]. The weak emitted signal at 423 K limits the measurement method below 5 μm. At higher temperature measurements, however, sample and environment temperatures become the main uncertainty sources at short and long wavelengths, respectively [19].

Fig. 4 shows the spectral emissivity curves of aluminum at 423 K and 823 K, for various values of the polar angle. In the case of metals, the emissivity rises with the angle, except around 90°, where it becomes zero after reaching a maximum [24]. The emissivity of metals is usually

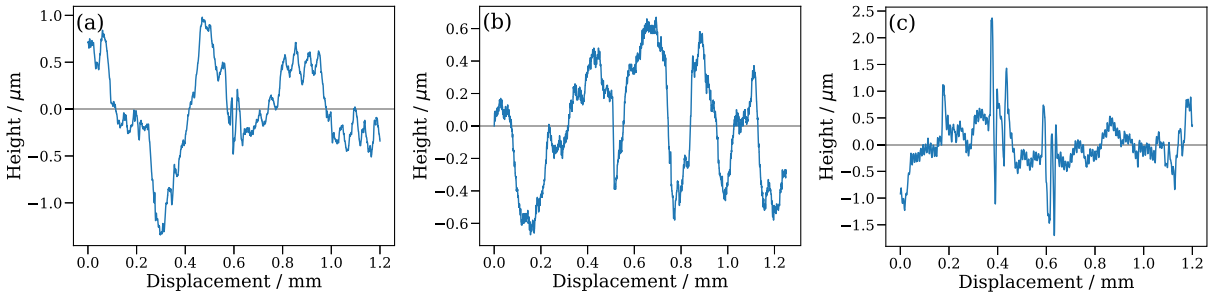

Fig. 1. Surface roughness profiles measured using a mechanical profilometer at (a) 0°, (b) 45°, and (c) 90° to the rolling direction.

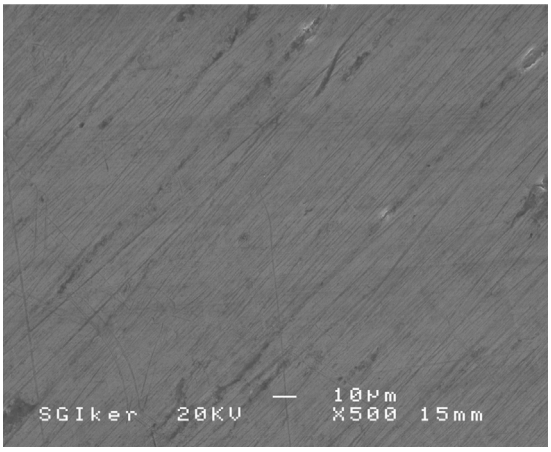

Fig. 2. Secondary electron SEM image of the sample surface, showing the rolling direction along the diagonal.

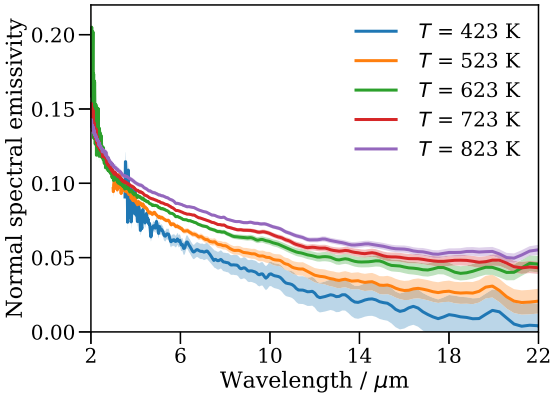

Fig. 3. Temperature-dependent near-normal (10°) emissivity spectra. Shaded regions correspond to standard uncertainties.

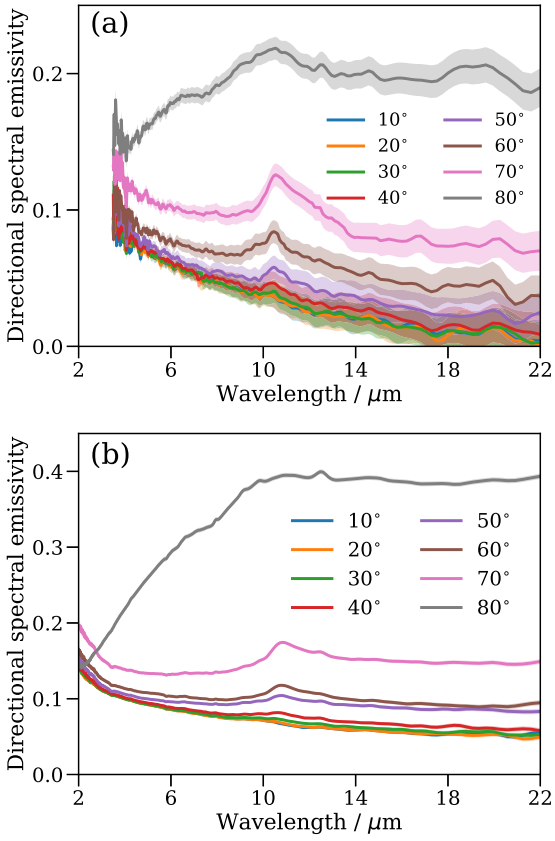

Fig. 4. Directional spectral emissivity measurements at (a) 423 K and (b) 823 K. Shaded regions correspond to standard uncertainties.

relatively constant until 40°, and then increases significantly with angle. Emissivity curves between 10° and 40° show a similar tendency, whereas for values above 50°, this tendency varies significantly, and the emissivity reaches higher values.

Despite having performed all measurements in a vacuum chamber, the appearance of an oxide layer in the sample surface is unavoidable. In this case, the presence of Al_2O_3 is noticeable due to the appearance of a local maximum at a value of about $\lambda = 11$ μm. This peak's origin can be explained by the Berreman effect, which describes the effect of longitudinal optical (LO) phonons on *p*-polarized reflectivities of thin polar layers on conducting substrates [26]. With the help of a linear polarizer, *s*- and *p*-polarized emissivity components were studied to ensure that the measurements are consistent with the Berreman effect. The results of directional spectral measurements of the two polarizations can be seen in Fig. 5. As expected, the peak can only be detected in the *p*-polarized data and becomes more apparent with increasing angle. The maximum of the peak is located at 10.8 μm, close to the literature value [27]. A similar peak has also been observed in normal spectral emissivity measurements of aluminum [8]. In that case, the intensity of the peak and its visibility in the normal direction pointed towards a much thicker oxide layer that grew with temperature.

An XPS analysis was performed to characterize the oxide layer and estimate its thickness, with the results shown in Fig. 6. The intensity of the peaks corresponding to the two chemical states of aluminum (Al^{3+} and Al^0) is represented in Fig. 6a at different points during depth profiling. At the surface, the peak corresponding to Al^{3+} is significantly higher than that of Al^0 (in blue). This tendency varies as the XPS test progresses and the deeper layers of the sample are studied. After a 60 min sputtering, at a depth of 31 nm, Al^0 appears in greater quantity, and Al^{3+} content is very small (in green). The total amount of aluminum and oxygen is shown in Fig. 6b as a function of depth. It can

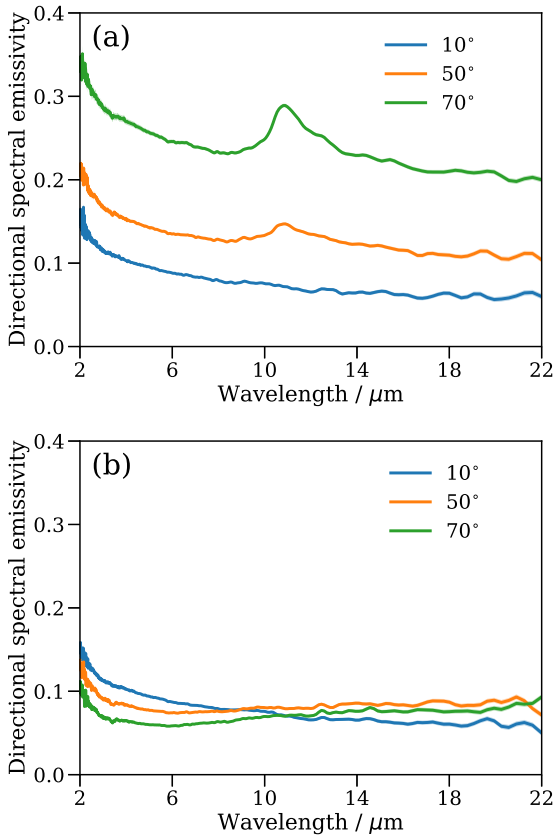

Fig. 5. Directional spectral emissivity measurements at 823 K measured in (a) *p* or (b) *s* polarization.

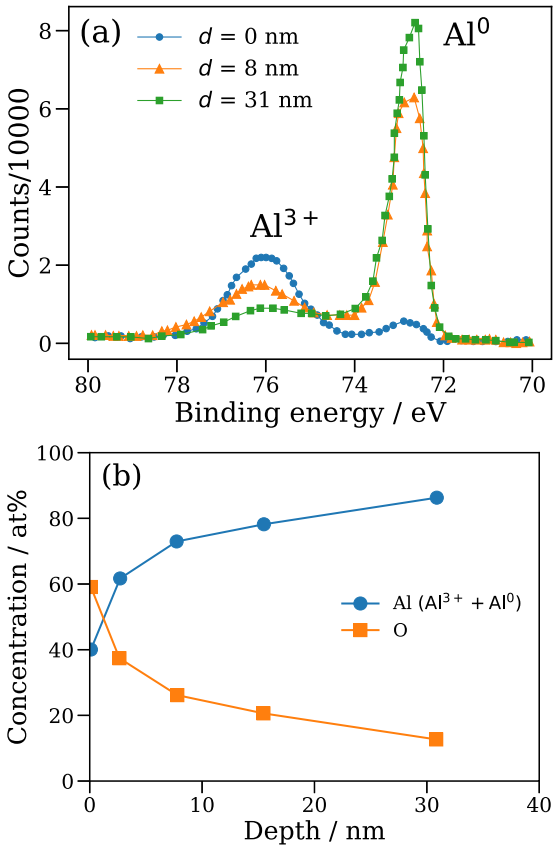

Fig. 6. XPS characterization of the sample after the emissivity measurements. (a) Spectrally resolved depth profile of the Al signals for the two oxidation states. (b) Depth profile of the integrated signals of Al and O, after calibration of the sputtering rate by comparison to a Ta_2O_5 reference.

be seen how almost no stoichiometric Al_2O_3 is present beyond the first nanometers of the sample, with the oxygen content decreasing quickly upon deeper penetration. The residual oxygen at depths greater than 10 nm can be attributed to the heterogeneous structure of the sample surface, rather than to dissolved oxygen [28].

3.2. Simulation results

Spectral emissivity data in the near-normal direction have been simulated as a function of temperature using the RCWA method described above. The simulated profile was based on the roughness measurements shown in Fig. 1b, which is representative of the average profile of the material in the normal direction. The anisotropic nature of the surface was not considered, as only near-normal results were simulated. To improve the quality of the simulations and remove any potential bias from enforcing periodic boundary conditions on a random structure, the profile was duplicated and inverted with respect to a mirror plane normal to the profilometer direction, thus extending the total length of the simulated profile (Fig. 7a).

Due to the computationally demanding nature of the RCWA algorithm, a complete numerical study could not be carried out with the resources available, especially with regards to the convergence of the algorithm. Because of these restrictions, the algorithm was run on 35 harmonics for all wavelengths and temperatures, while convergence tests were only implemented up to 45 harmonics in two cases, a worst- and a best-case scenario. The former consisted of the 523 K case at 22 μm, whereas the latter corresponded to 823 K and 2 μm. The criterion for selecting these points corresponds to the highest and lowest refractive-index contrast between the material and the incident medium (vacuum). The size of this mismatch is the key parameter behind the convergence rate of calculations on metallic gratings [29]. The results of this test are shown in Fig. 7b, and have been used to estimate an approximate relative error of 3% for all wavelengths when 35 harmonics are used.

The simulated emissivities are compared to near-normal experimental data in Fig. 8, together with the emissivities predicted by Fresnel's equations for an ideal surface [24]. The same dielectric function model was used for both calculations. The spectral emissivities predicted by the RCWA method are in good agreement with the experimental values, especially for the high temperature case. Not only has the quantitative value of the emissivity been calculated within a maximum relative error of 30%, but also the shape of the curve has been correctly estimated, showing an increase of the emissivity at short wavelengths. It must be noted that numerical simulations of electromagnetic scattering by pure metals in the infrared region are known to present convergence problems [29]. Although the calculations at 823 K seem accurate, those at 523 K hint at a possibly imperfect convergence. Therefore, even though a general error of 3% was estimated, it is possible that further evolution of the results takes place at higher numbers of harmonics for the lowest temperatures under study. As discussed before, the number of harmonics employed was limited by RAM capacity, given the large size of the simulated profile (100 layers). Further studies on the implementation and convergence rate of RCWA algorithms for the study of the emissivity of rough metals are required.

A comparison to the results predicted by Fresnel's equations shows the importance of accounting for surface roughness, even in samples with relatively low root-mean-square roughness values R_q, the traditional criterion for distinguishing near-specular surfaces from rougher ones [5,24]. The ideal surface approximation underestimates the emissivity of the sample at all wavelengths, not just at the shortest ones,

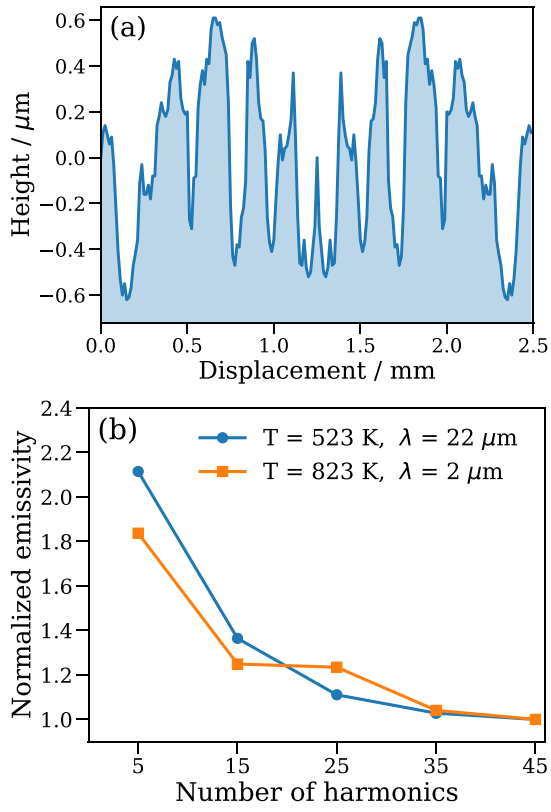

Fig. 7. (a) Repeating unit used in the RCWA calculations, obtained by discretizing the surface profile at 45° to the rolling direction and coupling it to its mirror image to enlarge its width. (b) Analysis of the convergence of two extreme cases, as a function of the number of harmonics.

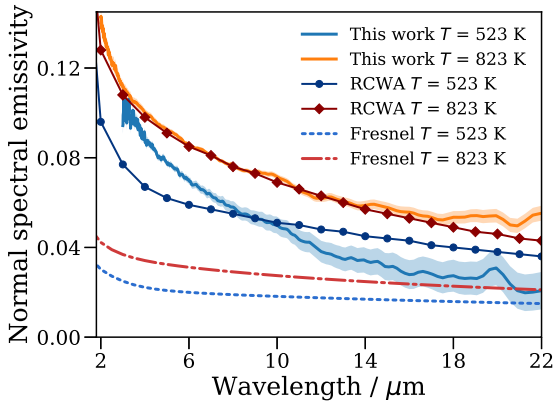

Fig. 8. Measurements of the emissivity values of aluminum at different wavelengths compared to theoretical data obtained by RCWA simulations of the measured profile and from Fresnel's equations (specular surface). The same optical data was used for both calculations [13].

where the relative size of roughness elements is greater. By contrast, the use of the RCWA method allows a direct simulation of the real state of the sample surface, including both the steeper valleys and the smaller roughness elements. Preliminary tests performed at lower resolution levels showed that the largest oscillations were by far the dominant scattering mechanism, and were responsible for a general increase in the emissivity at all wavelengths. Overall, it is shown that not only is RCWA a powerful tool to describe the emissivities of random surfaces which are characterized as neither near-specular nor belonging to the geometrical optics regime, but also that full simulations of real random

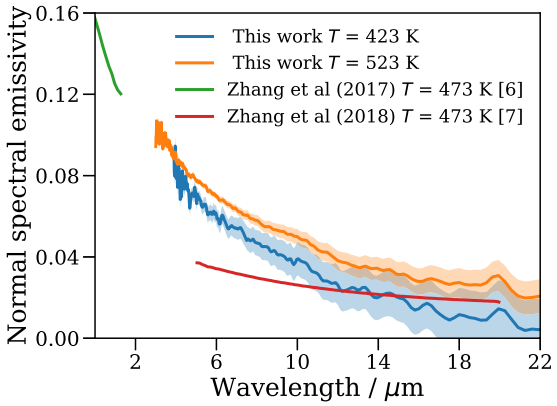

Fig. 9. Spectral emissivity values of aluminum compared to literature data at similar temperatures [6,7]. Shades correspond to standard uncertainties.

profiles can be implemented and used to accurately reproduce the observed features of the spectra. These results also support the idea that a precise surface characterization beyond the usual average parameters is essential to improve reproducibility of results among different studies. More work needs to be done to predict the emissivities of general surface profiles with varying roughness length scales, especially with regards to the directionality of emission and the anisotropic nature of rolled surfaces.

Future work will consider improvements such as parallelization of the code and the Fast Fourier Factorization implementation of RCWA [30]. New semianalytical methods specially designed to work with rough surfaces will also be considered [31]. Moreover, the role of the thin oxide layer will be investigated in more detail, to determine its potential effect on the emissivity beyond the Berreman peak and also its potential improvement of the convergence rate of the code, by easing the matching between layers with different refractive indices.

3.3. Comparison with literature data

As stated before, differences in surface state are the main responsible for discrepancies in literature data regarding the emissivity of pure aluminum. These references can be classified into those reporting normal spectral or total hemispherical values, measured using different techniques. In the case of normal spectral emissivity values, two sets of measurements on 99.6% pure Al in the near- and mid-infrared ranges were reported using measurement methods similar to the one used in this work [6,7]. A comparison with these data is shown in Fig. 9, where it can be seen that, despite both samples being similarly polished to $R_a \simeq 0.07$ μm and measured at the same temperature, notable differences can be seen in their spectral dependence. Whereas Ref. [7] shows values lower than the ones reported in this work, and more consistent with the Fresnel calculations shown in Fig. 8, the values reported in Ref. [6] are higher and with a steeper slope. It must be noted that the behavior of both data sets is consistent with the values reported in this work in the long- and short-wavelength limits of the measured spectral range, respectively. Thus, it is suggested that a characterization of surface states given only by the average roughness values is not sufficient to account for the entire influence of the surface in the emissivity of pure metals.

Other authors have reported monochromatic optical data at wavelengths relevant for laser processing, based on either measured data [3] or theoretical calculations [14]. These values can be used to obtain temperature-dependent emissivity data at $\lambda = 10.6$ μm, which are compared to the ones reported in this work, and the corresponding theoretical predictions, in Fig. 10. Data from the previously discussed multispectral study was added for completeness [7]. Although the emissivities reported by all sources show similar temperature dependences,

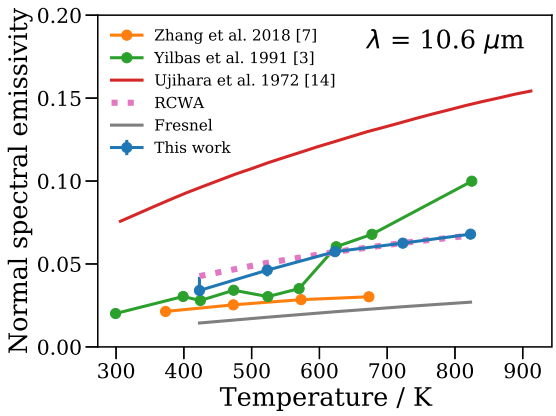

Fig. 10. Single-wavelength emissivity values of aluminum at different temperatures compared to the data found in literature [3,7,14], as well as to theoretical predictions reported in this paper for the Hüttner model [13] for specular (Fresnel) and rough (RCWA) surfaces.

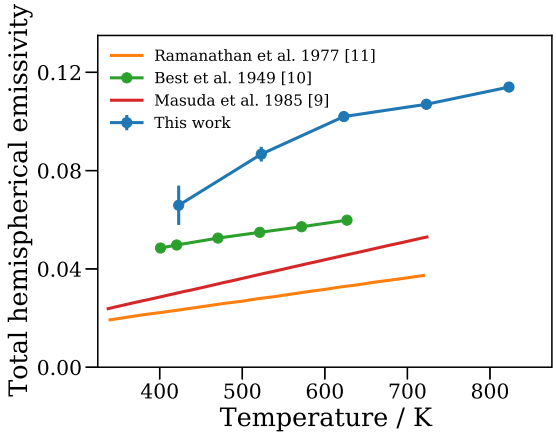

Fig. 11. Total hemispherical emissivity values at different temperatures compared to literature data obtained using calorimetric methods [9–11]. Error bars correspond to combined standard uncertainties.

there is considerable dispersion between the absolute values. Despite strong fluctuations, data reported by Yilbas et al. [3] is the closest to the measurements reported in this work, whereas the previously discussed data by Zhang et al. [7] are closest to the Fresnel limit for a specular surface. Once again, the accuracy of the RCWA calculations are worthy of note, especially at higher temperatures. Finally, the inadequacy of the Ujihara model of the optical properties of Al can be clearly observed [14], with values much larger than even those of rough surfaces. In this regard, the Hüttner model used in this work for both the Fresnel and RCWA calculations appears to be more accurate for the estimation of the emissivities of pure aluminum surfaces. A reason for this might be that, contrary to the Ujihara model, it relies extensively on measured data to estimate the temperature dependence of phenomenological parameters [13].

Finally, some references report only total hemispherical emissivity values of aluminum, which are determined using steady-state or transient calorimetric methods [9–11]. In order to compare the results in this work to these data, a numerical integration procedure was followed [19]. The results of this comparison are shown in Fig. 11, where a general disagreement between all data sets can be clearly observed. The main difference between the results in this work and those from the literature stems from the degree of polishing, as all three references report measurements on mechanically or electrolytically polished surfaces. Nevertheless, the disagreement for polished samples is also notable, and reinforces the idea that even relatively minor surface imperfections can drastically increase the emissivity of metals. It is worth noting the fact that the study performed by Ramanathan et al. is the only one where an electrolytically polished 99.999% pure sample was used, which can explain the fact that it features the lowest emissivity [11].

4. Conclusions

Directional spectral measurements of the infrared emissivity of a rolled sample of high-purity aluminum in the 423–823 K temperature range have been presented in this work. The presence of a polarized emission peak at oblique angles is associated to the Berreman effect, which is caused by the nanometric native oxide layer. The emissivity is shown to be heavily influenced by surface roughness in the entire mid-infrared range, even for mean roughness values that are much lower than the wavelengths under study. These influences can be approximately taken into account by RCWA calculations based on the surface profile obtained by a roughness tester. The use of a high-purity aluminum sheet in vacuum prevented potential confounding effects, leaving roughness as the main factor driving the increase in the emissivity. The multi-scale roughness features typical of rolled surfaces can affect the emissivity in complex ways, a phenomenon that can explain some of the discrepancies observed in literature data. More extensive work needs to be done to analyze the full polarized angular emission characteristics of these materials for a variety of surface states, especially considering their anisotropic nature and the potential dependence of the polarized directional emissivity on the polar and azimuthal angles. Finally, numerical studies on randomly rough surfaces with greater computing power or more optimized algorithms will be pursued.

Declaration of competing interest

The authors declare that they have no known competing financial interests or personal relationships that could have appeared to influence the work reported in this paper.

Data availability

Data will be made available on request.

Acknowledgments

This work was funded by the University of the Basque Country, Spain (GIU19/019) and the Basque Government, Spain (IT-1714-22 and PIBA-2021-1-0022). J. Gabirondo-López and I. González de Arrieta also acknowledge financial support from pre- and post-doctoral fellowships by these institutions (University of the Basque Country, Spain: PIF 21/06; Basque Government, Spain: POS-2021-2-0022). Technical support was provided by the SGIker service of UPV/EHU for the XPS analysis. Finally, the authors thank Jordan Edmunds for assistance with the RCWA code.

References

[1] M.J. Haugh, Radiation thermometry in the aluminum industry, in: D.P. DeWitt, G.D. Nutter (Eds.), Theory and Practice of Radiation Thermometry, John Wiley & Sons, Hoboken, New Jersey, 1988, pp. 905–971.

[2] R. Usamentiaga, P. Venegas, J. Guerediaga, L. Vega, J. Molleda, F.G. Bulnes, Infrared thermography for temperature measurement and non-destructive testing, Sensors 14 (7) (2014) 12305–12348.

[3] B.S. Yilbas, K. Danisman, Z. Yilbas, Measurement of temperature-dependent reflectivity of Cu and Al in the range 30–1000 °C, Meas. Sci. Technol. 2 (7) (1991) 668.

[4] C.D. Wen, I. Mudawar, Emissivity characteristics of polished aluminum alloy surfaces and assessment of multispectral radiation thermometry (MRT) emissivity models, Int. J. Heat Mass Transfer 48 (7) (2005) 1316–1329.

[5] C.-D. Wen, I. Mudawar, Modeling the effects of surface roughness on the emissivity of aluminum alloys, Int. J. Heat Mass Transfer 49 (23–24) (2006) 4279–4289.
[6] K. Zhang, K. Yu, Y. Liu, Y. Zhao, Effect of surface oxidation on emissivity properties of pure aluminum in the near infrared region, Mater. Res. Express 4 (8) (2017) 086501.
[7] K. Zhang, Y. Zhao, K. Yu, Y. Liu, Development of experimental apparatus for precise emissivity determination based on the improved method compensating disturbances by background radiation, Infrared Phys. Technol. 92 (2018) 350–357.
[8] P.M. Reynolds, Spectral emissivity of 99.7% aluminium between 200 and 540 °C, Br. J. Appl. Phys. 12 (3) (1961) 111.
[9] H. Masuda, M. Higano, Transient calorimetric technique for measuring total hemispherical emissivities of metals with rigorous evaluation of heat loss through thermocouple leads, J. Opt. Soc. Amer. A 2 (11) (1985) 1877–1882.
[10] G. Best, Emissivities of copper and aluminum, J. Opt. Soc. Amer. 39 (12) (1949) 1009–1011.
[11] K.G. Ramanathan, S.H. Yen, E.A. Estalote, Total hemispherical emissivities of copper, aluminum, and silver, Appl. Opt. 16 (11) (1977) 2810–2817.
[12] N.W. Ashcroft, K. Sturm, Interband absorption and the optical properties of polyvalent metals, Phys. Rev. B 3 (6) (1971) 1898.
[13] B. Huttner, Optical properties of polyvalent metals in the solid and liquid state: aluminium, J. Phys.: Condens. Matter 6 (13) (1994) 2459.
[14] K. Ujihara, Reflectivity of metals at high temperatures, J. Appl. Phys. 43 (5) (1972) 2376–2383.
[15] J.L. King, H. Jo, S.K. Loyalka, R.V. Tompson, K. Sridharan, Computation of total hemispherical emissivity from directional spectral models, Int. J. Heat Mass Transfer 109 (2017) 894–906.
[16] M.G. Moharam, T.K. Gaylord, Rigorous coupled-wave analysis of planar-grating diffraction, J. Opt. Soc. Amer. 71 (7) (1981) 811–818.
[17] Z.M. Zhang, Nano/Microscale Heat Transfer, in: Mechanical Engineering Series, vol. 410, Springer, 2007.
[18] J. Qiu, W.J. Zhang, L.H. Liu, P.-f. Hsu, L.J. Liu, Reflective properties of randomly rough surfaces under large incidence angles, J. Opt. Soc. Amer. A 31 (6) (2014) 1251–1258.
[19] I. González de Arrieta, T. Echániz, R. Fuente, J.M. Campillo-Robles, J.M. Igartua, G.A. López, Updated measurement method and uncertainty budget for direct emissivity measurements at the University of the Basque Country, Metrologia 57 (4) (2020) 045002.
[20] K. Yu, G. Wang, L. Li, K. Zhang, Y. Liu, A new experimental apparatus for polarized spectral emissivity measurement in a controlled environment, Infrared Phys. Technol. 111 (2020) 103572.
[21] L. Li, K. Yun, K. Zhang, Y. Liu, F. Zhang, Y. Liu, Accuracy improvement for directional polarized spectral emissivity measurement in the wavelength range of 4–20 μm, Exp. Therm Fluid Sci. 125 (2021) 110379.
[22] J. Edmunds, edmundsj/rcwa: Beta Release v0.1.125, Zenodo, 2022, http://dx.doi.org/10.5281/zenodo.6344979.
[23] T. Echániz, I. González de Arrieta, A. Gil-Muñoz, J. Fernández-Pereda, R. Fuente, M. Klimenkov, G.A. López, Infrared emissivity of reduced-activation Eurofer 97 for fusion reactor applications, J. Nucl. Mater. 549 (2021) 152907.
[24] J.R. Howell, M.P. Mengüç, R. Siegel, Thermal Radiation Heat Transfer, fifth ed., CRC Press, Boca Raton, 2010.
[25] I. Setién-Fernández, T. Echániz, L. González-Fernández, R.B. Pérez-Sáez, M.J. Tello, Spectral emissivity of copper and nickel in the mid-infrared range between 250 and 900 °C, Int. J. Heat Mass Transfer 71 (2014) 549–554.
[26] D.W. Berreman, Infrared absorption at longitudinal optic frequency in cubic crystal films, Phys. Rev. 130 (6) (1963) 2193.
[27] M. Kaltchev, W.T. Tysoe, An infrared spectroscopic investigation of thin alumina films: measurement of acid sites and surface reactivity, Surf. Sci. 430 (1–3) (1999) 29–36.
[28] J. Zähr, S. Oswald, M. Türpe, H.J. Ullrich, U. Füssel, Characterisation of oxide and hydroxide layers on technical aluminum materials using XPS, Vacuum 86 (9) (2012) 1216–1219.
[29] B. Caballero, A. García-Martín, J.C. Cuevas, Generalized scattering-matrix approach for magneto-optics in periodically patterned multilayer systems, Phys. Rev. B 85 (24) (2012) 245103.
[30] H. Mohamad, S. Essaidi, S. Blaize, D. Macias, P. Benech, A. Morand, Fast Fourier factorization for differential method and RCWA: a powerful tool for the modeling of non-lamellar metallic diffraction gratings, Opt. Quantum Electron. 52 (2) (2020) 1–13.
[31] Z. Zhu, C. Zheng, VarRCWA: An adaptive high-order rigorous coupled wave analysis method, ACS Photonics 0 (2022) null, http://dx.doi.org/10.1021/acsphotonics.2c00662.